Authors
Maria B Lai, Chi Zhang, Jianli Shi, Verity Johnson, Lavan Khandan, John McVey, Michael W Klymkowsky, Zhe Chen, and Harald J Junge

Article

Cell Reports

TSPAN12 Is a Norrin Co-receptor that Amplifies Frizzled4 Ligand Selectivity and Signaling

Graphical Abstract

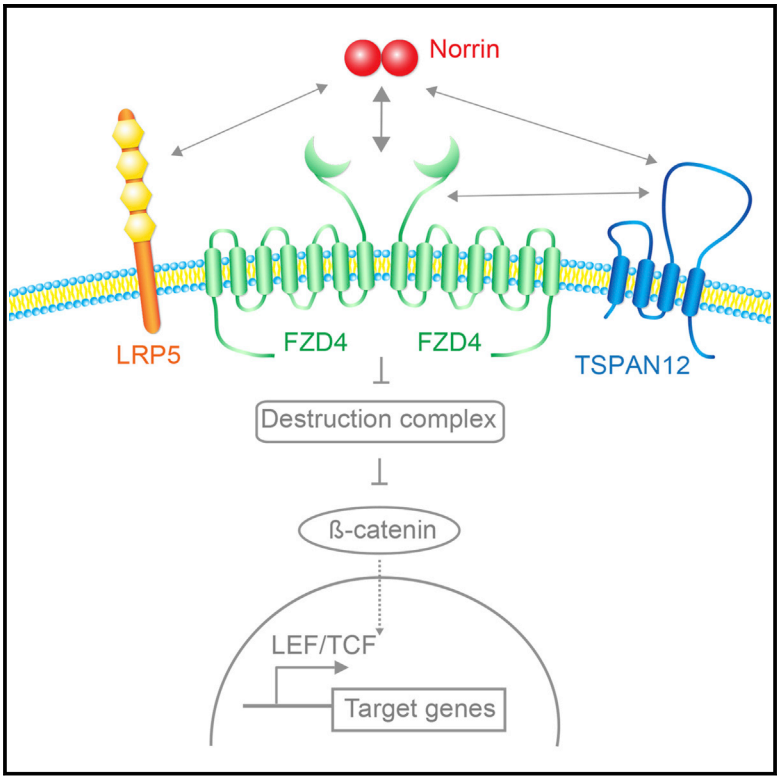

Authors

Maria B. Lai, Chi Zhang, Jianli Shi, ..., Michael W. Klymkowsky, Zhe Chen, Harald J. Junge

Correspondence

harald.junge@colorado.edu

In Brief

Lai et al. study the role of tetraspanin12 in the norrin receptor complex, which mediates canonical frizzled4 signaling in retinal angiogenesis and is involved in familial exudative vitreoretinopathy. Using mutational approaches, cell-based assays, and in vivo experiments, the authors show that tetraspanin12 stabilizes norrin/frizzled4 complexes and increases ligand selectivity of frizzled4.

Highlights

- Disease-linked missense mutations impair tetraspanin12 function
- Tetraspanin12 trafficking is promoted by frizzled4
- Tetraspanin12 interacts with norrin and frizzled4
- Tetraspanin12 stabilizes the ligand/receptor complex and enhances signaling in vivo

Lai et al., 2017, Cell Reports *19*, 2809–2822
June 27, 2017
http://dx.doi.org/10.1016/j.celrep.2017.06.004

Cell Reports
Article

TSPAN12 Is a Norrin Co-receptor that Amplifies Frizzled4 Ligand Selectivity and Signaling

Maria B. Lai,[1] Chi Zhang,[1] Jianli Shi,[1] Verity Johnson,[1,2] Lavan Khandan,[1] John McVey,[1,3] Michael W. Klymkowsky,[1] Zhe Chen,[1] and Harald J. Junge[1,4,*]
[1]Department of Molecular, Cellular, and Developmental Biology, University of Colorado, Boulder, CO 80309, USA
[2]Present address: ArcherDx, Boulder, CO 80301, USA
[3]Present address: Cleveland Clinic Lerner College of Medicine, Cleveland, OH 44195, USA
[4]Lead Contact
*Correspondence: harald.junge@colorado.edu
http://dx.doi.org/10.1016/j.celrep.2017.06.004

SUMMARY

Accessory proteins in Frizzled (FZD) receptor complexes are thought to determine ligand selectivity and signaling amplitude. Genetic evidence indicates that specific combinations of accessory proteins and ligands mediate vascular β-catenin signaling in different CNS structures. In the retina, the tetraspanin TSPAN12 and the ligand norrin (NDP) mediate angiogenesis, and both genes are linked to familial exudative vitreoretinopathy (FEVR), yet the molecular function of TSPAN12 remains poorly understood. Here, we report that TSPAN12 is an essential component of the NDP receptor complex and interacts with FZD4 and NDP via its extracellular loops, consistent with an action as co-receptor that enhances FZD4 ligand selectivity for NDP. FEVR-linked mutations in TSPAN12 prevent the incorporation of TSPAN12 into the NDP receptor complex. In vitro and in *Xenopus* embryos, TSPAN12 alleviates defects of FZD4 M105V, a mutation that destabilizes the NDP/FZD4 interaction. This study sheds light on the poorly understood function of accessory proteins in FZD signaling.

INTRODUCTION

A multitude of metazoan developmental processes are controlled by wnt/β-catenin signaling, a central signaling pathway that is perturbed in human diseases, including cancer, bone disease, and vascular disease (Clevers and Nusse, 2012). Canonical β-catenin signaling is mediated by a diverse group of ligands, receptors, co-receptors, and accessory co-activators. Core components of receptor complexes are frizzled receptors and low-density lipoprotein receptor-like protein 5/6 (LRP5 or LRP6) co-receptors, which inactivate the β-catenin destruction complex in order to regulate transcription (MacDonald and He, 2012). The combinatorial assembly of receptor complexes from multiple additional families of membrane proteins is thought to provide ligand selectivity and contribute to context-specific signaling outcomes (van Amerongen and Nusse, 2009). Despite their important roles, the function of accessory proteins in determining ligand-receptor selectivity and the mechanisms of receptor complex assembly are poorly understood (Schulte, 2015).

The critical in vivo role of distinct ligands and specific accessory membrane proteins in β-catenin signaling is particularly evident in CNS blood vessel development and blood-CNS barrier formation, processes that require canonical β-catenin signaling in endothelial cells (Liebner et al., 2008; Wang et al., 2012; Ye et al., 2009; Zhou et al., 2014). While WNT7A and WNT7B have critical roles in neural tube angiogenesis (Stenman et al., 2008), retinal signaling is mediated by the ligand NDP (norrie disease protein, also referred to as norrin). The cysteine-knot protein NDP acts through only one of the ten human FZD receptors, FZD4 (Smallwood et al., 2007). Unlike canonical WNT/FZD signaling, NDP/FZD4 signaling requires an additional membrane protein, the tetraspanin TSPAN12. Gene disruptions of *Tspan12* (Junge et al., 2009), *Ndp* (Luhmann et al., 2005), *Fzd4* (Xu et al., 2004; Ye et al., 2009), and *Lrp5* (Xia et al., 2008) all result in similar ocular phenotypes in mice, characterized by defects in intraretinal capillary development and dysregulation of the blood-retina barrier. NDP has been studied in several disease models for its vascular and neuroprotective roles (Chen et al., 2015; Ohlmann and Tamm, 2012).

Genetic experiments indicate that specific combinations of ligands and accessory proteins are predominantly required in some CNS structures. This is best illustrated by comparing the postnatal retina and the midgestation neural tube, each at time points of active angiogenesis and barriergenesis. NDP and TSPAN12 (Junge et al., 2009; Luhmann et al., 2005) have essential functions in the retina (i.e., functions not masked by redundancy), whereas WNT7A/B and the co-activator GPR124 carry out important functions in the neural tube (Posokhova et al., 2015; Stenman et al., 2008; Zhou and Nathans, 2014). Because TSPAN12 enhances NDP-induced but not WNT7A/B-induced signaling (Junge et al., 2009), whereas GPR124 enhances WNT7A/B-induced but not NDP-induced signaling (Posokhova et al., 2015; Zhou and Nathans, 2014), the accessory proteins are candidates for mediating ligand selectivity of receptor complexes containing FZD. However, biochemical evidence for this concept is largely lacking. TSPAN12 (of the tetraspanin family) and GPR124 (of the adhesion GPCR [G-protein-coupled

receptor] family) have distinct structures and characteristics; e.g., GPR124 appears to function together with another membrane molecule, RECK (Ulrich et al., 2016; Vanhollebeke et al., 2015). Available crystal structures of NDP in complex with the extracellular domain of FZD4 show that a NDP head-to-tail dimer contacts two FZD4 molecules (Chang et al., 2015; Shen et al., 2015). The residues in the interaction interface are well defined and overlap with disease-associated mutations in NDP and FZD4. FZD4 residues that contact NDP are, in part, conserved in other FZDs (especially in FZD9 and FZD10), but no FZD other than FZD4 harbors all residues that interact with NDP. Accessory proteins may enhance ligand selectivity, but how they assemble into receptor complexes and whether they contribute to ligand binding are not known.

The 33 human tetraspanin family members function in diverse biological processes and are implicated in several human diseases. TSPAN12, for example, is implicated in cancer (Knoblich et al., 2014; Otomo et al., 2014). Despite the interest in this protein family, the molecular basis of tetraspanin activity remains incompletely understood (Charrin et al., 2014).

Impaired NDP/FZD4 signaling in humans causes the retinal vascular disease FEVR (familial exudative vitreoretinopathy). Mouse genetic and human genetic studies (Junge et al., 2009; Nikopoulos et al., 2010a; Poulter et al., 2010) revealed the critical function of TSPAN12 in NDP/FZD4 signaling and FEVR, which is characterized by an avascular peripheral retina and other anomalies that may cause blindness (Gilmour, 2015; Kashani et al., 2014a). FEVR can be caused by mutations in *NDP*, *FZD4*, *LRP5*, *TSPAN12*, and *ZNF408*—a zinc finger protein recently implicated in vascular biology (Collin et al., 2013; Nikopoulos et al., 2010b). *TSPAN12* mutations have been predominantly reported in autosomal dominant FEVR (Kashani et al., 2014b; Kondo et al., 2011; Nikopoulos et al., 2010a; Poulter et al., 2010; Yang et al., 2011 Xu 14) but also in homozygous patients with an autosomal recessive inheritance pattern (Gal et al., 2014; Poulter et al., 2012; Savarese et al., 2014).

Here, we focus on the role of TSPAN12 in mediating ligand selectivity in FZD4 signaling. Our data support a model in which TSPAN12 functions in the NDP receptor complex as a co-receptor for NDP, facilitates selective ligand recognition, and enhances NDP/FZD4 signaling strength to a level that is required for normal retinal angiogenesis and blood-retina barrier function. We confirm the link between *TSPAN12* and FEVR by showing that FEVR-linked TSPAN12 mutations fail to incorporate into the NDP receptor complex.

RESULTS

TSPAN12 Missense Mutations Impair FZD4 Signaling in a Ligand-Specific Manner

We introduced ten previously identified FEVR-linked missense mutations (Kondo et al., 2011; Nikopoulos et al., 2010a; Poulter et al., 2010, 2012; Yang et al., 2011) individually into hemagglutinin (HA)-tagged TSPAN12 (Figures 1A and S1). When we compared the TOPFlash reporter activity (Veeman et al., 2003) of 293T cells transfected with FZD4, LRP5, and wild-type TSPAN12 versus mutated TSPAN12, we found that the ability of TSPAN12 to enhance NDP/FZD4 signaling was impaired to various degrees by the FEVR-linked mutations. C105R, M210R, L223P, A237P, and L245P strongly impaired TSPAN12 activity; T49M, L101H, and Y138C mildly impaired TSPAN12 activity; and G188R and L201F were functionally similarly to wild-type in TOPFlash assays (Figure 1B). To further assess functional impairment of TSPAN12 mutations, we used a NDP C95R rescue assay (Junge et al., 2009). As expected, cells stimulated with co-transfected NDP C95R showed only marginal reporter activity, but overexpression of TSPAN12 resulted in substantial rescue of NDP C95R-associated signaling defects (Figure 1C). This assay revealed defects of G188R and L201F mutations that were not apparent with stimulation by wild-type NDP (Figure 1B).

When we induced signaling with WNT7B or WNT3A, we observed no TSPAN12-mediated signaling enhancement or detrimental effect of TSPAN12 missense mutations, indicating that sufficient FZD4 reached the cell surface when TSPAN12 with missense mutations was co-expressed (Figures 1D and 1E). These results are consistent with a ligand-specific role of TSPAN12 in FZD4 signaling. The strong reduction of NDP induced signaling by the C105R, M210R, L223P, A237P, and L245P mutations confirms the positive role of TSPAN12 in NDP/FZD4 signaling and validates a causal link between TSPAN12 mutations and FEVR.

Several TSPAN12 Missense Mutations Impair Cell Surface Localization and Cause Poor Association with the NDP Receptor Complex

NDP is a high-affinity ligand for FZD4 and can be used to isolate FZD4 and associated proteins from the plasma membrane (Junge et al., 2009; Xu et al., 2004). To determine whether FEVR-linked TSPAN12 mutations affect the association of TSPAN12 with the NDP receptor complex, we transfected 293T cells with FZD4 and TSPAN12 (wild-type or mutated), incubated live cells with cold FLAG-AP-NDP conditioned medium (CM) (i.e., an alkaline phosphatase fusion protein), and then isolated NDP and associated plasma membrane proteins. As expected, FZD4 and TSPAN12 co-immunoprecipitated with NDP; however, several of the mutant TSPAN12 proteins exhibited poor association with the NDP receptor complex and reduced expression levels (Figures 2A and 2C). The binding defects were more severe than expression defects and, for most mutations, correlated well with the extent of functional defects observed in TOPFlash assays. The five mutations that caused the strongest signaling defects in TOPFlash assays (C105R, M210R, L223P, A237P, and L245P) also exhibited very poor association with NDP and FZD4. Some discrepancies between signaling and binding defects were observed for the G188R mutation; a possible explanation for this difference is the presence of detergent in the biochemical assay, which may exacerbate binding defects.

To determine whether mutant TSPAN12 proteins traffic to the plasma membrane, we performed surface biotinylation experiments using live 293T cells transfected with HA-TSPAN12 constructs. C105R, L223P, A237P, and L245P strongly impaired surface localization (Figures 2B and 2D). Together, these results indicate that plasma membrane localization of TSPAN12 and association with the NDP receptor complex are required for its function in NDP/FZD4 signaling.

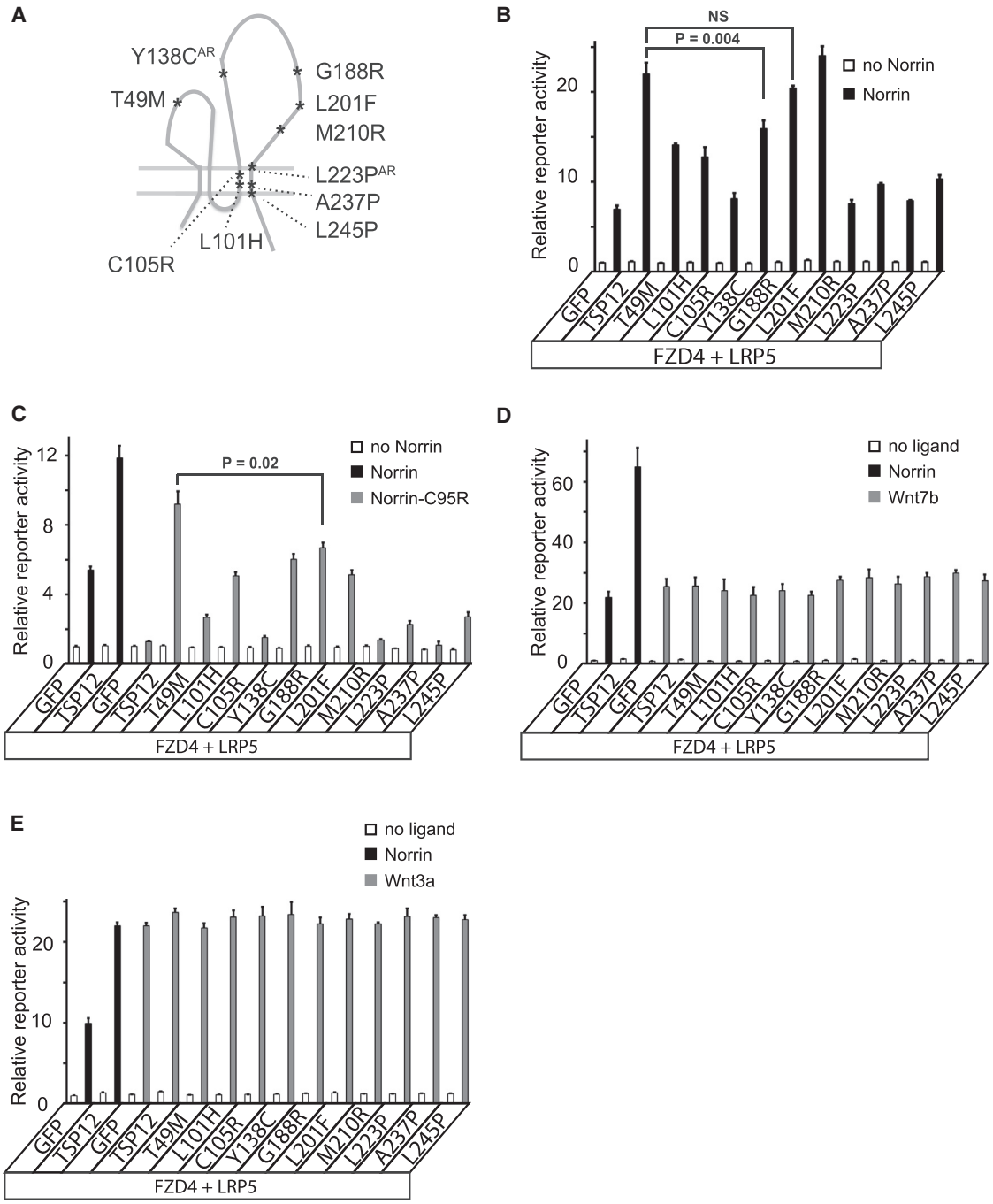

Figure 1. FEVR-Linked TSPAN12 Mutations Impair NDP/FZD4 but Not WNT/FZD Signaling

(A) Schematic overview of the position of FEVR-linked point mutations in TSPAN12. AR, autosomal recessive.

(B) TOPFlash assay induced with 125 ng/mL recombinant NDP. Mutations affect TSPAN12 activity to various degrees. NS, not significant.

(C) Functional impairment of TSPAN12 mutations was examined in a NDP-C95R rescue experiment. NDP expression vectors were co-transfected to induce signaling.

(D) No functional impairment of FEVR-linked TSPAN12 mutations in WNT7B/FZD4 signaling.

(E) No functional impairment of FEVR-linked TSPAN12 mutations in WNT3A/FZD signaling. NDP, WNT3A, and WNT7B expression vectors were co-transfected to induce signaling.

All panels: n = 3; error bars indicate mean + SD.

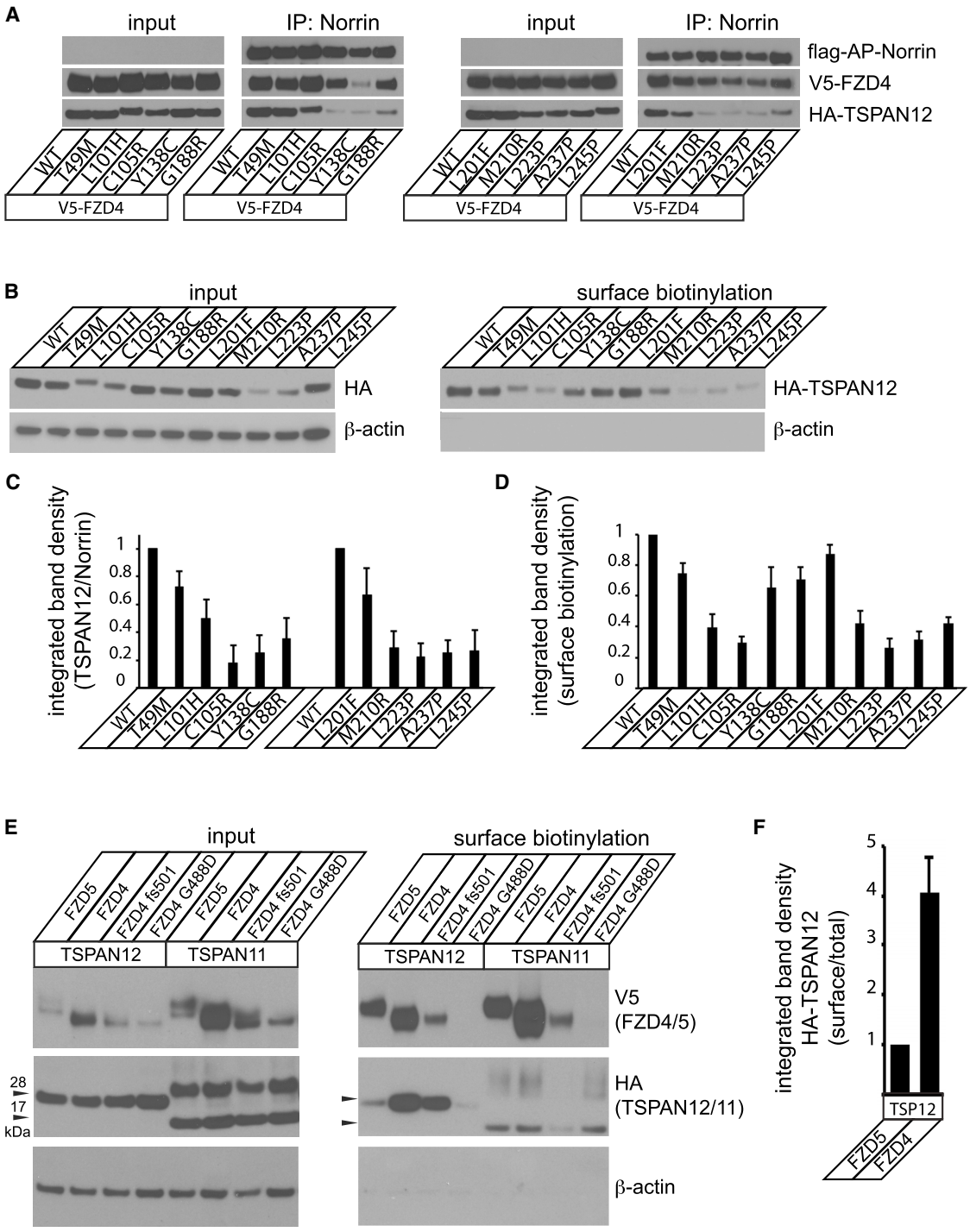

Figure 2. FEVR-Linked TSPAN12 Mutations Impair the Association of TSPAN12 with the NDP Receptor Complex and Trafficking to the Plasma Membrane

(A) Live cells expressing V5-FZD4 and HA-TSPAN12 were incubated with FLAG-AP-NDP conditioned medium before ligand-associated proteins were immunoprecipitated. TSPAN12 proteins with mutations co-precipitate with NDP and FZD4 to various degrees. Note that NDP concentrations in the diluted lysate are below the detection limit using standard detection systems. NDP is, however, strongly enriched using anti-FLAG beads and is clearly detectable in the bead eluates. IP, immunoprecipitate; WT, wild-type.

(B) 293T cells were transfected as indicated, and plasma membrane proteins of live cells were biotinylated. Cells were lysed, and a fraction of the lysate was loaded (input). Biotinylated proteins were isolated with Neutravidin beads and probed with anti-HA antibody (surface biotinylation). Mutations affect TSPAN12 surface expression to various degrees.

(legend continued on next page)

FZD4 Strongly Promotes TSPAN12 Transport to the Plasma Membrane

In the previously described experiments, we consistently observed that TSPAN12 Y138C overexpression caused a reduction in the amount of FZD4 that is immunoprecipitated with NDP (Figure 2A). Cell-surface biotinylation experiments revealed that localization of both FZD4 and FZD5 at the plasma membrane was reduced in the presence of TSPAN12 Y138C, compared to wild-type TSPAN12 (Figure S2). Next, we analyzed the co-dependence of FZD4 and TSPAN12 in trafficking. Wild-type TSPAN12 (compared to TSPAN11) did not promote FZD4 transport to the cell surface; rather, it slowed its transport (Figure 2E). Conversely, we found that FZD4 (compared to FZD5) strongly promoted TSPAN12 trafficking to the cell surface (Figures 2E and 2F; see also Figure 4B). To rule out that the difference was caused by inhibitory effects of FZD5, we utilized ER (endoplasmic reticulum)-resident FZD4 variants FZD4 fs501X533 and FZD4 G488D (Kaykas et al., 2004; Milhem et al., 2014), which strongly impaired transport of co-transfected TSPAN12 to the plasma membrane. In contrast, control tetraspanin TSPAN11, which was detected in two major bands, was transported to the surface to a similar degree in the presence of FZD4, FZD4 G488D, or FZD5. Only FZD4 fs501x533 impaired surface localization of both TSPAN12 and TSPAN11, suggesting non-specific defects in FZD4 fs501x533-expressing cells. The findings imply that the NDP receptor complex is at least partially assembled in the absence of NDP during intracellular trafficking and that TSPAN12 transport to the plasma membrane is strongly promoted by FZD4.

The Large Extracellular Loop of TSPAN12 Is Required for Enhancing NDP-Induced FZD4 Signaling

To test whether the interaction of TSPAN12 and FZD4 is functionally required, we screened for useful tools using a chimera approach. We chose TSPAN11 as a donor tetraspanin, because it has the same number of cysteine residues (six) in the large extracellular loop (LEL; Figure S3) and because NDP/FZD4 signaling output is inert toward TSPAN11 (see Figure 3B). We created a series of chimeras in which the N terminus ($TSPAN12^{11\text{-}NT}$), the C terminus ($TSPAN12^{11\text{-}CT}$), the individual transmembrane segments ($TSPAN12^{11\text{-}TM1}$, etc.), and the small extracellular loop (SEL) and LEL ($TSPAN12^{11\text{-}SEL}$ and $TSPAN12^{11\text{-}LEL}$) of TSPAN12 were replaced by corresponding TSPAN11 sequences (Figure 3A). Of this set of chimeras, we sought to identify those that display functional impairment but intact cell-surface localization. TOPFlash assays revealed that the intracellular N terminus of TSPAN12 is not required for function, and replacing the intracellular C terminus caused only a partial reduction in signaling. The chimeras harboring the SEL and the LEL of TSPAN11, as well as several chimeras with exchanged transmembrane segments (TM2, TM3, and TM4), lost the ability to enhance NDP/FZD4 signaling (Figure 3B). None of the chimeras affected WNT7B-induced FZD4 signaling, indicating that sufficient FZD4 reached the cell surface in the presence of chimera co-expression (Figure 3C).

We performed cell-surface biotinylation experiments to test whether chimeras were functionally impaired due to altered cell-surface expression (Figure 3D) and selected $TSPAN12^{11\text{-}LEL}$, which was efficiently transported to the surface, for further analysis. Immunoblots for cell-surface TSPAN11 showed a band at ≈16 kDa and a smear above 30 kDa due to a modification, which we identified as N-glycosylation during the course of this study (Figure 4D). This modification was carried over to the $TSPAN12^{11\text{-}LEL}$ chimera. The finding that the $TSPAN12^{11\text{-}LEL}$ chimera localizes to the plasma membrane at high levels, but does not enhance NDP/FZD4 signaling, suggests that essential protein-protein interactions are disrupted.

TSPAN12 Is Anchored to the NDP Receptor Complex via an Interaction of the LEL with FZD4

NDP co-immunoprecipitation experiments showed that TSPAN12, $TSPAN12^{11\text{-}NT}$, and $TSPAN12^{11\text{-}CT}$ were incorporated into the NDP receptor complex, whereas $TSPAN12^{11\text{-}LEL}$ failed to associate with the complex (Figure 4A). To test whether $TSPAN12^{11\text{-}LEL}$ /FZD4 interactions are disrupted during intracellular transport, we assayed FZD4-dependent trafficking of TSPAN12 to the plasma membrane (Figure 4B). While wild-type TSPAN12, $TSPAN12^{11\text{-}NT}$, and, to a lesser degree, $TSPAN12^{11\text{-}CT}$ chimeras showed increased transport to the cell surface in the presence of FZD4 as expected (Figure 2E), surface expression of the $TSPAN12^{11\text{-}LEL}$ chimera was not increased by FZD4 co-expression. Next, we used an anti-V5 antibody to label V5-FZD4 on the plasma membrane of live cells and isolated FZD4 plus associated proteins from the cell surface. While TSPAN12, $TSPAN12^{11\text{-}NT}$, and $TSPAN12^{11\text{-}CT}$ co-immunoprecipitated with FZD4 as expected, $TSPAN12^{11\text{-}LEL}$ did not interact with FZD4 (Figure 4C). FZD4 association of the negative control TSPAN12 A237P, which resides mostly in intracellular compartments (Figure 2B), was hardly detectable. To rule out that post-translational modification of the TSPAN11 LEL prevented FZD4 binding to $TSPAN12^{11\text{-}LEL}$, we mutated two predicted N-glycosylation sites in TSPAN11—i.e., N127 and N159—and found that both were post-translational modification sites. When N-glycosylation of $TSPAN12^{11\text{-}LEL\ N127S,\ N159S}$ was prevented, the chimera was still unable to bind FZD4 (Figure 4D). Next, we determined whether the extracellular regions of TSPAN12 were sufficient to mediate FZD4 binding. $TSPAN11^{12\text{-}SEL,\ LEL}$ (i.e., the TSPAN11 tetraspanin scaffold with both extracellular loops of TSPAN12; Figure 4E) was sufficient to mediate FZD4 binding (Figure 4F). This interaction did not require endogenous LRP5

(C) Integrated band density quantification of TSPAN12 co-precipitated with Norrin as shown in (A) (n = 3 independent experiments; error bars indicate mean + SD).
(D) Integrated band density quantification of cell-surface TSPAN12, as shown in (B) (n = 3 independent experiments; error bars indicate mean + SD).
(E) Surface biotinylation experiment using 293T cells transfected with the indicated expression vectors. TSPAN12 surface expression is strongly promoted by FZD4. FZD4 fs501x533 partially traps TSPAN12 and TSPAN11 unspecifically in intracellular compartments. FZD4 G488D reduces TSPAN12 transport specifically. Two N-glycosylation sites are predicted in the control tetraspanin TSPAN11 (see also Figure 4D).
(F) Integrated band density quantification of cell-surface TSPAN12 relative to total TSPAN12 in the presence of FZD4 or FZD5 (n = 3 independent experiments; error bars indicate mean + SD).

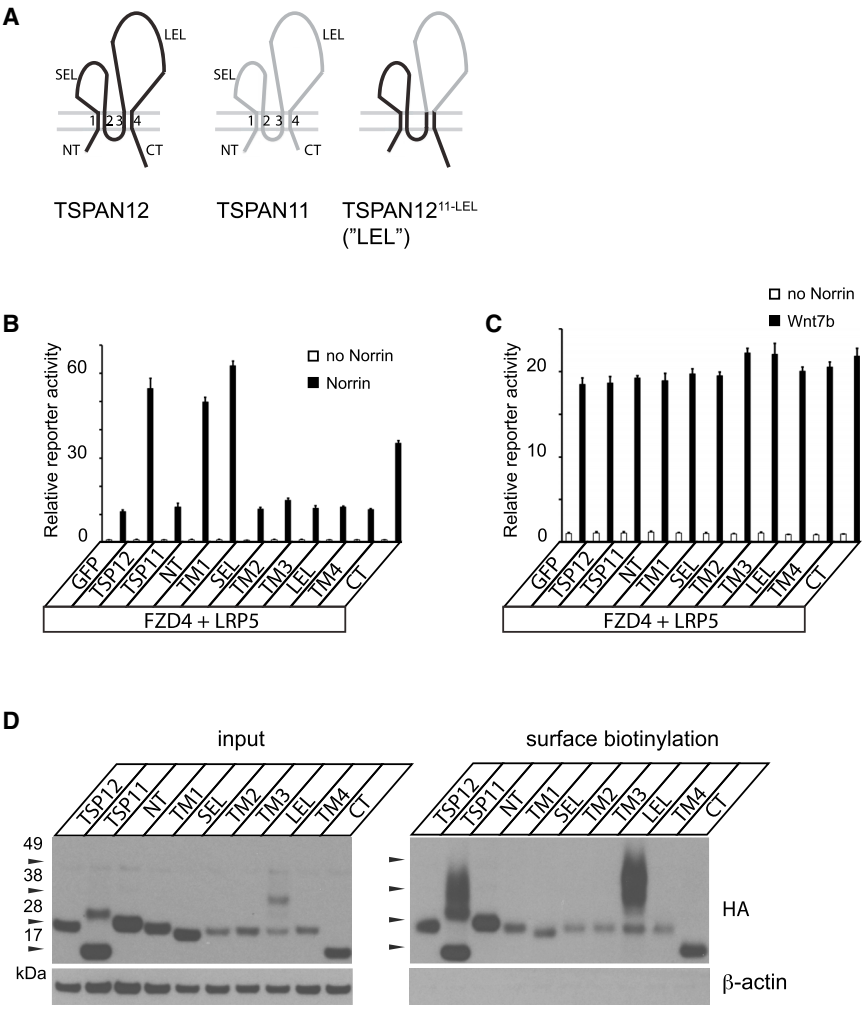

Figure 3. TSPAN12$^{11\text{-}LEL}$ Is Efficiently Transported to the Cell Surface but Is Not Functional in NDP/FZD4 Signaling

(A) Schematic representation of TSPAN12 sequence segments that were individually exchanged against corresponding TSPAN11 sequences to generate chimeras. The TSPAN12$^{11\text{-}LEL}$ chimera is depicted, for example. SEL, small extracellular loop; LEL, large extracellular loop; NT, N terminus; CT, C terminus.

(B and C) TOPFlash assay transfected with the indicated plasmids (n = 3; error bars indicate mean + SD).

(D) 293T cells transfected with the indicated expression vectors were subjected to cell-surface biotinylation. Note that the post-translational modification site of TSPAN11 is carried over to the TSPAN12$^{11\text{-}LEL}$ chimera (see also Figure 4D).

or -6 (Figure 4G), which were deleted using CRISPR/Cas9 (Figure S4). These observations support a model in which TSPAN12 is anchored to the Norrin receptor complex via its LEL.

TSPAN12 Extracellular Loops Are Sufficient to Interact with NDP

TSPAN12 functions in the NDP receptor complex and enhances FZD4 signaling in a ligand-specific manner. These findings raise the possibility that TSPAN12 is a co-receptor that binds NDP. To test whether TSPAN12 interacts with NDP, we performed NDP co-immunoprecipitations of TSPAN12 in the absence of FZD4. Cell-surface binding of NDP in the absence of FZD4 was reduced (Figure 5A, top right panel), and remaining cell-surface binding was, in part, mediated by unknown proteins expressed in 293T cells. Because it was not possible to clearly differentiate the contribution of TSPAN12 to cell-surface binding in the presence of other NDP-binding proteins, we used immunoprecipitation experiments and appropriate negative controls to test for NDP binding to TSPAN12. Cell-surface-bound NDP co-precipitated TSPAN12, whereas negative controls TSPAN12$^{11\text{-}LEL}$ and TSPAN12 A237P were clearly excluded from the immunoprecipitate (Figure 5A). The absence of TSPAN12$^{11\text{-}LEL}$ in the co-immunoprecipitate was not due to N-glycosylation of the LEL, as TSPAN12$^{11\text{-}LEL\ N127S,\ N159S}$ also did not interact with NDP (Figure 5B). To further test the specificity of the NDP/TSPAN12 interaction, we used NDP C55R, a mutant with signaling defects that are only minimally rescued by TSPAN12 co-expression (Figure 5C). Whereas wild-type NDP co-precipitated TSPAN12 in the absence of FZD4, no interaction between NDP C55R and TSPAN12 was detected (Figure 5D). Due to difficulties expressing TSPAN12 extracellular regions without a tetraspanin transmembrane scaffold, we were unable to test whether the interaction of NDP and TSPAN12 is direct. Thus, we used CRISPR/Cas9-mediated gene targeting to remove *FZD4*, or *LRP5* and *LRP6*, from 293T cells, which were processed through a single-cell stage (Figures S4 and S5). TSPAN12 interacted with NDP in the absence of endogenous FZD4 or endogenous LRP5/6. The extracellular regions of TSPAN12 in TSPAN11$^{12\text{-}SEL,\ LEL}$ (i.e., the TSPAN11 tetraspanin scaffold with both extracellular loops of TSPAN12; see Figure 4E) were sufficient to mediate the interaction with NDP, albeit at reduced levels (Figures 5E and 5F). These observations are consistent with a model in which TSPAN12 extracellular loops are contact points for both the FZD4 receptor and the NDP ligand.

TSPAN12 Restores NDP/FZD4 Binding and Signaling when the NDP/FZD4 Interaction Is Perturbed by Mutations

To test the functional significance of the interaction of NDP and TSPAN12, we used mutations in FZD4 and NDP that each weaken the interaction of the receptor with the ligand. FZD4 M105V showed significantly reduced signaling induced by either NDP or, to a lesser degree, WNT7B. Co-expression of TSPAN12

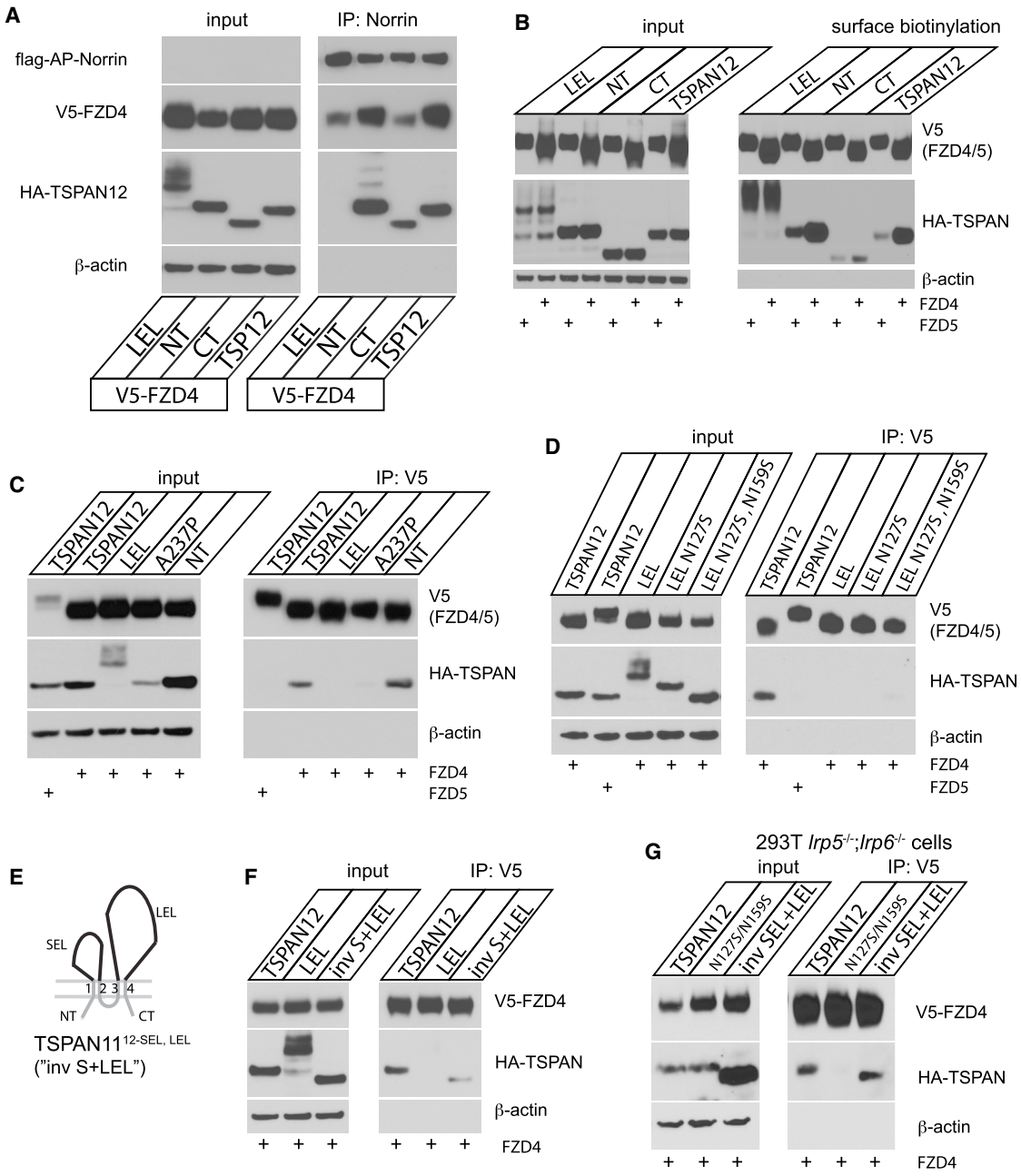

Figure 4. TSPAN12 Extracellular Loops Are Necessary and Sufficient for the Interaction with FZD4

(A) NDP co-immunoprecipitation after FLAG-AP-NDP binding to intact cells transfected with the indicated expression vectors. TSPAN12$^{11\text{-}LEL}$ is not co-precipitated. IP, immunoprecipitate; NT, N terminus; CT, C terminus.

(B) 293T cells were transfected as indicated, and plasma membrane proteins of intact cells were biotinylated. FZD4 promotes the transport of TSPAN12; TSPAN12$^{11\text{-}NT}$; and, to a lesser extent, TSPAN12$^{11\text{-}CT}$ to the cell surface, whereas surface expression of TSPAN12$^{11\text{-}LEL}$ is FZD4-independent.

(C) Intact cells expressing V5-FZD4 and HA-TSPAN12 were incubated with anti-V5 antibody. FZD4 or FZD5 and associated proteins were immunoprecipitated using protein A/G beads. FZD4 co-precipitates TSPAN12 and TSPAN12$^{11\text{-}NT}$, whereas FZD5 does not interact with TSPAN12. TSPAN12$^{11\text{-}LEL}$ does not interact with FZD4, and only trace amounts of TSPAN12 A237P are detected in the eluate.

(D) Identification of two N-glycosylation sites in TSPAN11. When N-glycosylation is prevented in TSPAN12$^{11\text{-}LEL\ N127S,\ N159S}$, the chimera remains unable to interact with FZD4.

(E) Schematic representation of the inverse chimera (inv S + LEL) carrying the TSPAN12 extracellular loops on a TSPAN11 tetraspanin scaffold.

(F) Immunoprecipiatation of cell-surface-bound V5 antibody shows that the extracellular loops of TSPAN12 are sufficient to mediate FZD4 binding, albeit at reduced levels.

(G) TSPAN12 interacts with FZD4 in the absence of endogenous LRP5/6.

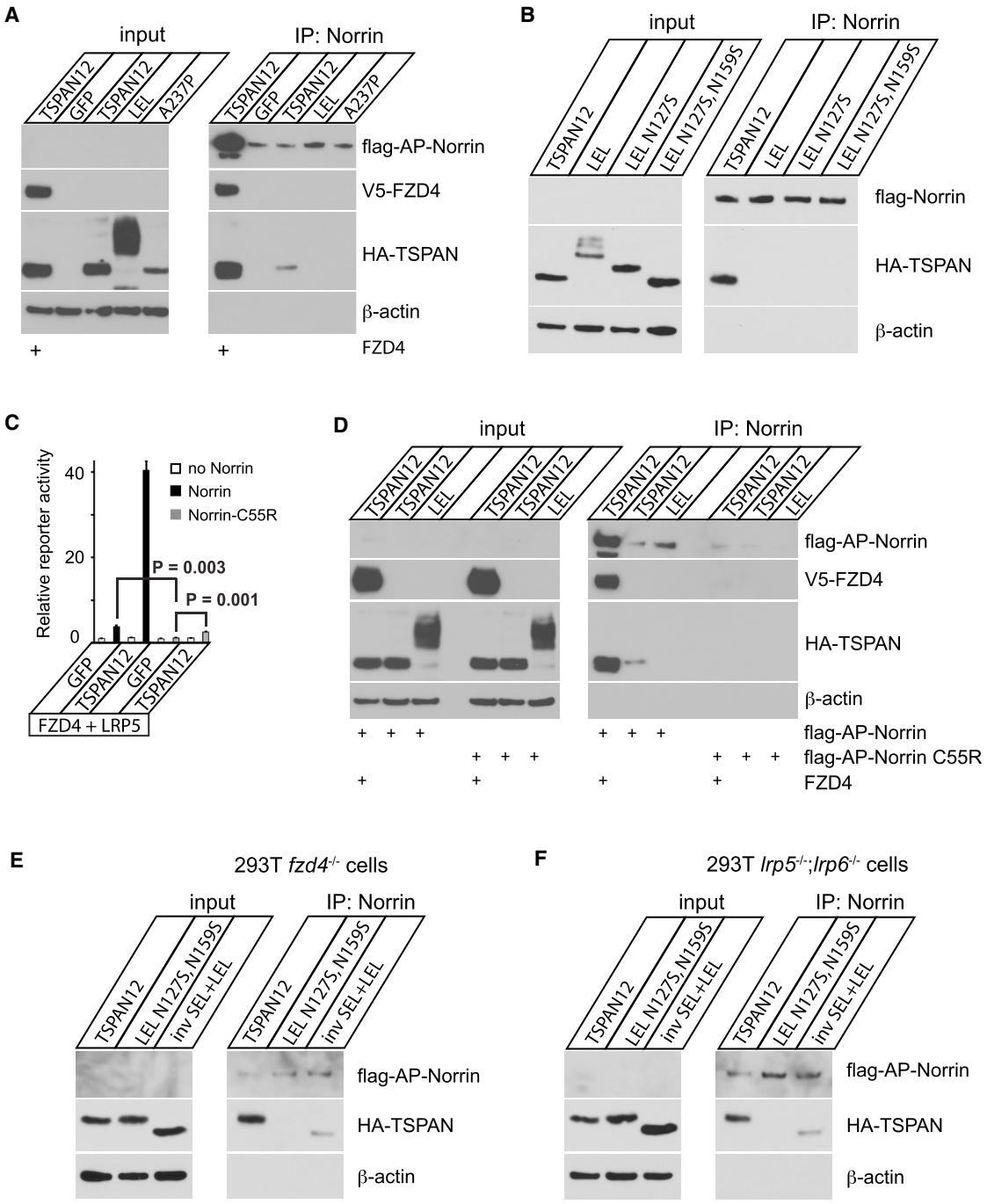

Figure 5. TSPAN12 Interacts with NDP in the Absence of FZD4 or LRP5/6

(A) NDP co-immunoprecipitation after FLAG-AP-NDP binding to intact cells. TSPAN12 co-precipitates with cell-surface-bound NDP; TSPAN12 co-precipitation is increased in the presence of FZD4. IP, immunoprecipitate.

(B) TSPAN12$^{11\text{-}LEL}$ and N-glycosylation-deficient TSPAN12$^{11\text{-}LEL\ N127S,\ N159S}$ do not interact with NDP.

(C) Functional impairment of NDP C55R in signaling was examined in TOPFlash assays (n = 3; error bars indicate mean + SD). Conditioned medium normalized for the content of FLAG-AP-NDP or FLAG-AP-NDP C55R was added to induce signaling.

(D) FLAG-AP-NDP binding to intact cells transfected with the indicated expression vectors. TSPAN12 co-precipitates with NDP but not with NDP C55R.

(E and F) TSPAN12 interacts with Norrin in the absence of (E) endogenous FZD4 or (F) endogenous LRP5/6. The extracellular portions of TSPAN12 are sufficient to interact with NDP in the context of the TSPAN11$^{12\text{-}SEL,LEL}$ chimera (see Figure 4E), albeit at a reduced level. inv, inverse.

largely rescued the signaling defects when signaling was induced by NDP; however, it had no effect on the signaling defects in WNT7B/FZD4 M105V signaling (Figure S6). Restoring impaired NDP/FZD4 M105V signaling required the LEL of TSPAN12, as TSPAN12$^{11\text{-LEL}}$ was not able to rescue signaling (Figure 6A). We confirmed previous results (Qin et al., 2008) showing that FZD4 M105V—which is in the NDP/FZD4 binding interface (Chang et al., 2015; Shen et al., 2015)—weakens the interaction with NDP, and we found that the binding defect is more readily revealed with more stringent washing, indicating that the mutation impairs the stability of NDP/FZD4 complexes. When we isolated NDP and associated plasma membrane proteins, we found that NDP was initially retained on the cell surface of FZD4- or FZD4 M105V-expressing cells so that it could subsequently be immunoprecipitated (Figure 6B, top right). However, NDP/FZD4 M105V failed to form a stable enough complex in the detergent extract; therefore, FZD4 M105V could not be detected in the co-precipitate. The stability of NDP/FZD4 complexes was greatly increased in the presence of wild-type TSPAN12, whereas TSPAN12$^{11\text{-LEL}}$, TSPAN12 A237P, and TSPAN12 M210R failed to restore NDP/FZD4 M105V binding. In support of these data, we found that HeLa cells expressing wild-type (WT) FZD4 M105V showed few proximity ligation amplification products (PLAPs) after incubation with NDP, while co-expression of WT TSPAN12 rescued FZD4/NDP complex formation (Figures 6C and 6D).

Impaired NDP binding as a mechanism of the FZD4 M105V signaling defect was further supported by experiments in which signaling was induced in a ligand-independent manner using a forced interaction approach. Tandem DmrA domains (engineered variants of the FKBP domain of FKBP12) were fused to the C terminus of FZD4, tandem DmrC domains (FRB domains of FRAP) were fused to the C terminus of LRP5, and the interaction was induced by A/C heterodimerizer (a derivative of rapamycin) in TOPFlash assays. Induction of the interaction resulted in NDP-independent stimulation of signaling, and this signaling component was not affected by the M105V mutation. The NDP-independent component of signaling induced by forced FZD4 and LRP5 heterodimerization was not enhanced by TSPAN12 (Figure S7).

To further test the role of TSPAN12 in stabilizing NDP/FZD4 complexes, we analyzed NDP R41E binding to FZD4, a mutation that substantially weakens the interaction of NDP and FZD4 (Smallwood et al., 2007). In addition, the crystal structures highlight that R41 contacts FZD4 (Chang et al., 2015; Shen et al., 2015). TOPFlash assays showed that NDP R41E displayed a strong signaling defect, which was partially rescued by the co-expression of TSPAN12 (Figure 6E). Immunoprecipitations of plasma-membrane-bound NDP indicated that NDP R41E was retained at the cell surface at reduced levels (Figure 6F, top right) and that NDP R41E was unable to co-precipitate FZD4. However, co-expression of TSPAN12 restored the NDP R41E/FZD4 interaction. Proximity ligation assays (PLAs) confirmed that TSPAN12 promotes NDP R41E binding to FZD4 on the cell surface of HeLa cells (Figures 6G and 6H). We also observed that TSPAN12 promotes the binding of WT NDP to FZD4 (Figures 4A and 6F). This function was most clearly revealed when the negative control was TSPAN$^{11\text{-LEL}}$ (see Discussion about the difference of GFP versus TSPAN$^{11\text{-LEL}}$ co-transfection and the effects on FZD4 expression levels).

TSPAN12 Enhances NDP-Induced Axis Duplication in Frog Embryos

Activation of β-catenin signaling in vertebrate embryos results in anterior-posterior axis duplication (Funayama et al., 1995; Kelly et al., 1995; Kühl and Pandur, 2008). We found that injection of *FZD4* RNA into the ventral cells of four-cell-stage *Xenopus* embryos was not sufficient to induce axis phenotypes; however, co-injection of *FZD4* and *NDP* RNAs resulted in axis duplication (revealed by in situ hybridization for *sox3*) in 31% of embryos. The incidence of this phenotype was clearly increased by co-injection of *TSPAN12* mRNA (49% incidence of axis duplication). NDP and FZD4 M105V were poor mediators of axis duplication (7% incidence), but co-injection of *TSPAN12* mRNA strongly increased the incidence of axis duplication in *FZD4 M105V*- and *NDP*-expressing embryos to 19% (Figure 7). These in vivo findings are in good agreement with the observation that TSPAN12 restores the binding and signaling of NDP and FZD4 M105V. The observation that NDP and FZD4 induce a duplicate axis in frog embryos further adds to the evidence that NDP is a canonical ligand (Zhou et al., 2014).

Taken together, we observed that TSPAN12 interacts with NDP in the absence of endogenous FZD4 or LRP5/6 and that TSPAN12 restores NDP/FZD4 binding when the interaction is perturbed by mutations in either NDP or FZD4. In accordance with these findings, TSPAN12 also restores the signaling defects of the same mutations. Based on these data, we propose a new model in which TSPAN12 acts as an NDP co-receptor that enhances FZD4 ligand selectivity and amplifies signaling.

DISCUSSION

In order to understand ligand selectivity, biased signaling outcomes, and modulation of signaling kinetics/amplitude in a variety of signaling systems, it is critical to unravel the function of accessory proteins. NDP and WNT receptor complexes appear to use distinct accessory proteins to enhance signaling strength and increase ligand selectivity. In vivo, accessory proteins are indispensable for CNS angiogenesis and blood-CNS barrier formation in a brain-region-specific manner. Our study provides insight into the assembly of the NDP receptor complex, the critical role of the accessory protein TSPAN12 in enhancing the ligand selectivity and signaling amplitude of FZD4, and the defects of FEVR-linked TSPAN12 mutations in human disease.

Previous studies have identified FEVR-linked mutations in *TSPAN12* and excluded the presence of these mutations in ethnically matched control individuals. Our analysis shows that several of these mutations, indeed, impair NDP/FZD4 signaling, thus confirming the link between TSPAN12, FEVR, and NDP/FZD4 signaling. We observed that TSPAN12 mutant proteins (especially C105R, L223P, A237P, and L245P) are not efficiently transported to the plasma membrane. This finding suggests a disease mechanism involving reduced rates of transport and/or folding, possibly due to the effects of proline substitutions on the alpha-helix secondary structure in TM4 (L223P, A237P, and L245P). Similarly, a positive charge introduced by the C105R

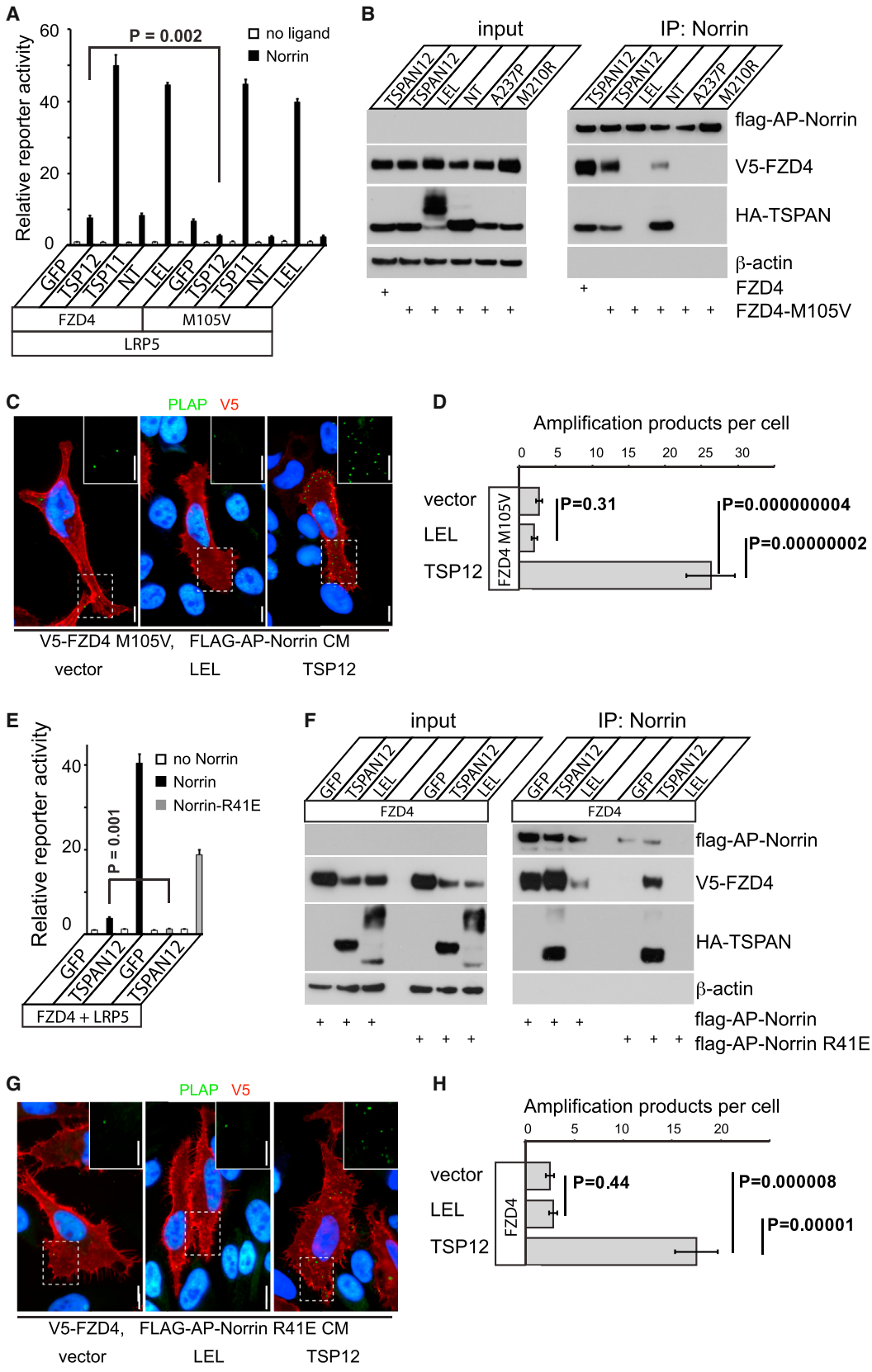

(legend on next page)

substitution could disrupt the conformation of TM3. These findings suggest that additional alleles, whose protein products modulate folding and membrane protein transport in endothelial cells, could be among the unknown modifiers of expressivity of FEVR-linked TSPAN12 mutations.

The mutual interactions of NDP receptor complex components in mediating cell-surface trafficking have previously not been studied. We observed that TSPAN12 transport to the plasma membrane is strongly increased by FZD4 (Figure 2E and 4B). We further characterized two FZD4 mutations that were previously reported to reduce FZD4 transport to the cell surface: FZD4 fs501x533 (Kaykas et al., 2004) and FZD4 G488D (Milhem et al., 2014), the latter specifically and severely reduces TSPAN12 transport to the plasma membrane. Our finding that FZD4 strongly promotes TSPAN12 trafficking implies that the NDP receptor complex is, at least partially, assembled during intracellular transport in the absence of NDP and that individual receptor complex components can strongly effect cell-surface localization of other components.

To test whether TSPAN12 functions in the NDP receptor complex, we utilized TSPAN12 chimeras carrying individual sequence segments of TSPAN11. This analysis yielded several insights: (1) the intracellular domains of TSPAN12 are not predominantly important for function, (2) the LEL of TSPAN12 is required for association with the NDP receptor complex via FZD4, and (3) TSPAN12 incorporation into the NDP receptor complex is required for TSPAN12 function. In light of a recent study reporting that TSPAN3 modulates NOGO-A/S1PR2 GPCR signaling (Thiede-Stan et al., 2015), it appears that tetraspanin activity and GPCR receptor signaling intersect in multiple biological contexts.

Current models of TSPAN12 function posit that TSPAN12 promotes FZD4 self-interactions (Junge et al., 2009) or FZD4/LRP5 hetero-interactions (Knoblich et al., 2014) to enhance β-catenin signaling. Alternatively, TSPAN12 may function as an allosteric modulator of FZD4 to increase signaling. These models are not mutually exclusive, and all are consistent with the requirement of TSPAN12 in retinal angiogenesis and the enhancement of signaling in cell-based assays. However, they provide little insight into the ligand-specific functions of TSPAN12 that are evident in cell-based assays and are supported by overlapping *tspan12*$^{-/-}$ and *ndp*$^{-/-}$ mouse mutant retinal phenotypes (Junge et al., 2009). With improved biochemical assays, we now show that TSPAN12 interacts with NDP in the absence of endogenous FZD4. A chimera composed of the TSPAN11 tetraspanin scaffold and the TSPAN12 extracellular loops is sufficient to bind both NDP and FZD4 (Figure 5). The function of TSPAN12 in modulating ligand binding to the receptor complex is particularly evident when the interaction of NDP and FZD4 is destabilized by the M105V mutation in the extracellular domain of FZD4 or the R41E mutation in NDP. In each case, NDP/FZD4 complexes are severely perturbed—consequently, signaling is strongly impaired—but co-expression of TSPAN12 stabilizes NDP/FZD4 complexes and significantly restores signaling (Figure 6). TSPAN12 also increases the co-precipitation of WT FZD4 with NDP (Figures 4A and 6F). We found that this effect is most clearly revealed when TSPAN12$^{11\text{-}LEL}$ is used as a negative control, because co-transfection of TSPAN11, GFP, or empty vector each results in increased FZD4 expression, compared to co-transfection of TSPAN12. TSPAN12 expression and transport are relatively inefficient, and when TSPAN12 binds to FZD4, the expression and transport of FZD4 are reduced (Figure 2E). Conversely, FZD4 expression and transport are highly efficient, and TSPAN12 transport to the cell surface is increased in complex with FZD4. The negative effect of TSPAN12 on FZD4 expression and transport tends to mask the positive effect of TSPAN12 in stabilizing the NDP/FZD4 interaction (Figure 6F).

We propose a model in which TSPAN12 serves as a co-receptor that promotes the ligand selectivity of FZD4, stabilizes NDP/FZD4 complexes, and enhances signaling to physiologically required levels. The requirement for TSPAN12 may be explained by the finding that NDP appears to bind only one site of FZD4 (site 2), whereas WNTs bind FZD via their lipid moiety also at site 1 (Chang et al., 2015; Janda et al., 2012; Shen et al., 2015). Our model is based on the following data: (1) phenotypic overlap of *tspan12*$^{-/-}$ and *ndp*$^{-/-}$ mice (in the retinal vasculature) and the absence of phenotypic overlap of *tspan12*$^{-/-}$ and *wnt7a; wnt7b* double-mutant mice (in the neural tube vasculature) (Junge et al., 2009); (2) ligand-specific functions of TSPAN12 in cell-based assays; (3) the function of TSPAN12 requiring incorporation into the NDP receptor complex; (4) TSPAN12-mediated restoration of binding and signaling defects caused by mutations in the NDP/FZD4 binding interface (FZD4 M105V and NDP R41E); and (5) TSPAN12/NDP binding in the absence of endogenous FZD4 or LRP5/6 (this interaction is mediated by the extracellular loops of TSPAN12). Possible

Figure 6. TSPAN12 Rescues Binding and Signaling Defects Caused by Mutations in the NDP/FZD4 Interface

(A) TOPFlash assay (n = 3; error bars indicate mean + SD). TSPAN12 and TSPAN12$^{11\text{-}NT}$, but not TSPAN12$^{11\text{-}LEL}$, rescue FZD4 M105V signaling defects.

(B) NDP co-immunoprecipitation after FLAG-AP-NDP binding to intact cells transfected with the indicated expression vectors. TSPAN12 increases FZD4 M105V co-precipitation with NDP.

(C) PLA in HeLa cells using primary anti-FLAG (to detect NDP) and anti-V5 (to detect FZD4 M105V, Alexa Fluor dye coupled) generates PLAPs (green puncta). Under stringent wash conditions, NDP binds FZD4 M105V poorly, but the complex is stabilized when TSPAN12 is co-transfected. Scale bars, 10 μm.

(D) Quantification of PLAPs (n = 37–42; error bars indicate mean + SEM shown).

(E) TOPFlash assay (n = 3; error bars indicate mean + SD). Conditioned medium normalized for the content of FLAG-AP-NDP (black bars) or FLAG-AP-NDP R41E (gray bars) was added to induce signaling.

(F) NDP and NDP R41E immunoprecipitation after binding to FZD4-expressing intact cells. TSPAN12 promotes FZD4 co-precipitation with NDP R41E. The quantity of NDP in the immunoprecipitate is a measure of cell-surface binding to FZD4-expressing cells. TSPAN12$^{11\text{-}LEL}$ co-transfection, compared to TSPAN12 co-transfection, results in similar FZD4 expression, whereas GFP co-transfection increases FZD4 expression.

(G) PLA in HeLa cells using primary anti-FLAG (to detect NDP R41E) and anti-V5 (to detect FZD4, Alexa Fluor dye coupled) generates PLAPs (green puncta). NDP R41E binds FZD4 poorly, but the complex is stabilized when TSPAN12 is co-transfected. Scale bars, 10 μm.

(H) Quantification of PLAPs (n = 20–28; error bars indicate mean + SEM).

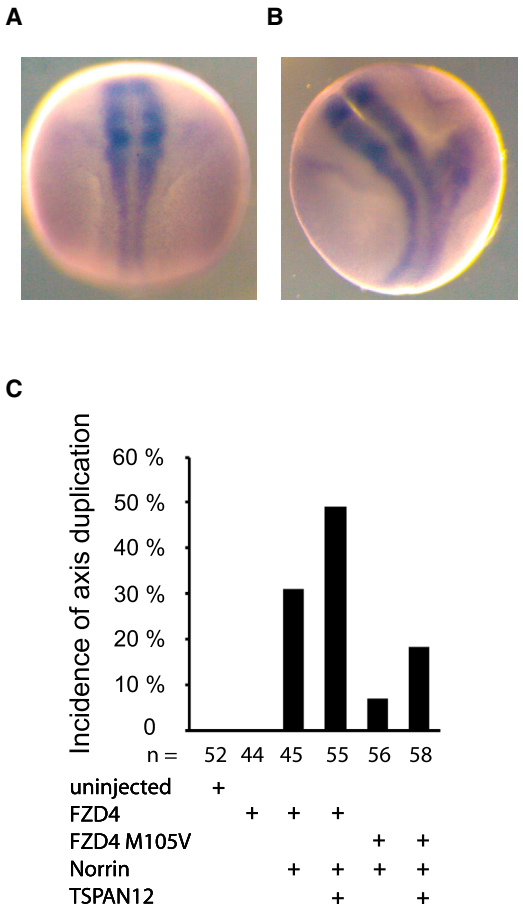

Figure 7. TSPAN12 Enhances NDP-Induced Axis Duplication in Frog Embryos

(A) Anterior-posterior axis in stage 18 control *Xenopus laevis* embryo revealed by in situ hybridization with a *sox3* probe.

(B) Axis duplication induced by *hNDP* and *hFZD4* RNA co-injection.

(C) 44–58 embryos per group were analyzed. Two independent experiments showed very similar results. Co-injection of *hTSPAN12* RNA increases the incidence of axis duplication in *hFZD4*- and *hFZD4* M105V-expressing embryos.

roles of TSPAN12 transmembrane domains include providing a scaffold that aids in the function of the extracellular loops, undergoing conformational changes upon ligand binding, contacting FZD4 for allosteric modulation, or engaging in tetraspanin-tetraspanin interactions for cell-membrane compartmentalization. When the NDP co-receptors TSPAN12 and LRP5 are compared, the evidence highlights a role for TSPAN12 in modulating ligand binding and ligand selectivity. Consistent with this view, the extracellular loops of TSPAN12 are functionally important. The predominant function of LRP5 in NDP signaling may be to engage the signal transduction machinery; this view is consistent with the intracellular protein interactions of LRP5 (Mao et al., 2001), as well as the finding that forcing the interaction of LRP5 and FZD4 using the FKBP system induces ligand-independent signaling (Figure S7). A limitation of our study is the inability to express extracellular portions of TSPAN12 without membrane domains, preventing us to formally test whether TSPAN12/NDP binding is direct. However, the finding that endogenous FZD4 or LRP5/6 in 293T cells are not required for this interaction is in agreement with our model.

Because canonical β-catenin signaling is required for angiogenesis and blood-CNS-barrier function in several CNS tissues, therapeutic intervention may allow the modulation of barrier properties for the purpose of drug delivery or treatment of ocular diseases. TSPAN12 appears to function predominantly in the retina, whereas FZD4 has broader functions both inside and outside the CNS, e.g., vital functions in the esophagus (Wang et al., 2001). Given the relatively tissue-specific but essential role of TSPAN12 in retinal angiogenesis, targeting this molecule may allow for inhibition of retinal neovascular diseases without broader CNS effects.

EXPERIMENTAL PROCEDURES

Plasmids

The generation of plasmid constructs by standard molecular biology techniques is described in the Supplemental Experimental Procedures.

Cell Culture

293T cells were cultured in high-glucose DMEM with 10% FBS at 37°C in the presence of 5% CO_2. For maintenance, cells were split 1:6 at near confluence using 0.05% Trypsin-EDTA.

TOPFlash Luciferase Assay

Detailed experimental procedures are described in the Supplemental Experimental Procedures. In brief, 293T cells were transiently transfected with receptor complex components, firefly-, and renilla-luciferase constructs. Cells were stimulated with recombinant NDP (R&D Systems) or by co-transfection of NDP or WNT plasmids. Dual-Glo luciferase assays (Promega) were performed. Data were analyzed by calculating the ratio of firefly/renilla luciferase signals and normalizing the data to the data point shown on the left of each bar graph in Figures 1B–1E, 3B, 3C, 5C, 6A, and 6E.

Generation of FLAG-AP-NDP Conditioned Medium

Detailed experimental procedures are described in the Supplemental Experimental Procedures. In brief, 293T cells were transiently transfected with FLAG-AP-NDP expression vector. The pH of conditioned medium was adjusted using 1 M HEPES, pH 8.0.

Co-immunoprecipitation

Detailed experimental procedures are described in the Supplemental Experimental Procedures. In brief, intact 293T cells on ice were incubated with cold FLAG-AP-NDP conditioned medium or with V5 antibody (AbD Serotec) in cold medium, washed, and lysed. FLAG-AP-NDP or V5 antibody bound to the receptor complex at the cell surface was isolated using anti-FLAG beads (Sigma) or Protein A/G Magnetic Beads (Pierce), respectively. Samples were analyzed by immunoblot.

Cell Surface Biotinylation Assay

Detailed experimental procedures are described in the Supplemental Experimental Procedures. In brief, intact 293T cells were placed on ice, washed with cold PBS (pH 8.0), and biotinylated with EZ-Link-Sulfo-NHS-SS-Biotin (Pierce). Excess reagent was removed, cells were lysed (yielding the "input" fraction), and biotinylated cell-surface proteins were isolated using High Capacity NeutrAvidin Agarose slurry (Pierce) (yielding the fraction "surface biotinylation"). Fractions were analyzed by immunoblot.

PLA

Detailed experimental procedures are described in the Supplemental Experimental Procedures. In brief, transfected HeLa cells were fixed and incubated with FLAG-AP-NDP conditioned medium, washed, and fixed again. Cells were

labeled with mouse anti-V5:Alexa Fluor 488 antibody (AbD Serotec) and rabbit anti-FLAG antibody (Sigma) in full medium. After washing, cells were incubated with anti-mouse and anti-rabbit PLA probes, i.e., secondary antibodies coupled to proprietary DNA oligonucleotides (Olink). DNA components of complementary PLA probes, if in sufficient proximity, were ligated. Fluorescent signal was generated using provided polymerase and substrate solutions according to manufacturer's instructions.

CRISPR/Cas9-Mediated Gene Targeting

293T cells were transfected with plasmids encoding Cas9 and short guide RNAs (sgRNAs) (deposited by Dr. Feng Zhang: Addgene #42230, co-transfected with GFP, or #62988, selected with puromycin). Individual colonies derived from single cells were picked and expanded. 293T cell clones were screened by genomic PCR. PCR products were analyzed after blunt ligation into pJet2.1 by sequencing ten individual bacterial clones. Clones were identified as positive if targeted alleles were null alleles and if a maximum of two types of targeted alleles was found, as expected from a single-cell-derived 293T cell clone. sgRNA sequences are shown in Figures S1–S7.

Frog Embryos, Their Manipulation and Analysis

*X. laevi*s embryos were manipulated following standard procedures. Capped mRNAs were transcribed using mMessage mMachine kits (Ambion), following the manual. At the four-cell stage, 150 pg of each RNA was injected at two ventral blastomeres. As an injection tracer, we routinely included RNAs (100 pg per embryo) encoding GFP, and embryos were examined at stages 10–11 by fluorescent microscopy to confirm the accuracy of injection. For whole-mount in situ hybridization studies, embryos were harvested at stage 18. Digoxigenin-UTP-labeled antisense probes were prepared using the Riboprobe Combination System (Promega) following the instructions; specific probes for *sox3* RNAs were used.

Statistics

Firefly and renilla luciferase activities were quantified as integrated luminescence output over 1 s. The ratio of firefly- to renilla-luciferase-generated luminescence was calculated. Averages of these ratios were calculated from triplicates. Immunoblot band intensities were quantified using the integrated density function of ImageJ from three independent experiments. Groups were compared using a two-tailed, unpaired Student's t test in Microsoft Excel. p values < 0.05 were considered significant.

SUPPLEMENTAL INFORMATION

Supplemental Information includes Supplemental Experimental Procedures and seven figures and can be found with this article online at http://dx.doi.org/10.1016/j.celrep.2017.06.004.

AUTHOR CONTRIBUTIONS

M.B.L., C.Z., Z.C., J.S., V.J., J.M., M.W.K., and H.J.J. designed experiments; M.B.L., C.Z., J.S., V.J., L.K., J.M., and H.J.J. conducted experiments and analyzed data; M.B.L. and H.J.J. wrote the manuscript.

ACKNOWLEDGMENTS

We would like to thank Davide Proverbio and Teodor Aastrup at Attana Research Services and Systems and Jana Valnohova and Gunnar Schulte at Karolinska Institutet for sharing unpublished data on the application of Quartz Crystal Microbalance technology to study ligand receptor interactions. We would also like to thank Dr. Paul Muhlrad for providing critical comments on the manuscript. This work was supported by ACS IRG #57-001-53 from the American Cancer Society (to H.J.J.), a Boettcher Foundation Webb-Waring Biomedical Research Award (to H.J.J.), a grant from the NIH (R01EY024261 to H.J.J.), and the Linda Crnic Institute (to M.W.K.).

Received: April 27, 2016
Revised: March 29, 2017
Accepted: May 27, 2017
Published: June 27, 2017

REFERENCES

Chang, T.H., Hsieh, F.L., Zebisch, M., Harlos, K., Elegheert, J., and Jones, E.Y. (2015). Structure and functional properties of Norrin mimic Wnt for signalling with Frizzled4, Lrp5/6, and proteoglycan. eLife *4*, e06554.

Charrin, S., Jouannet, S., Boucheix, C., and Rubinstein, E. (2014). Tetraspanins at a glance. J. Cell Sci. *127*, 3641–3648.

Chen, Y., Zhang, Y., Tang, J., Liu, F., Hu, Q., Luo, C., Tang, J., Feng, H., and Zhang, J.H. (2015). Norrin protected blood-brain barrier via frizzled-4/β-catenin pathway after subarachnoid hemorrhage in rats. Stroke *46*, 529–536.

Clevers, H., and Nusse, R. (2012). Wnt/β-catenin signaling and disease. Cell *149*, 1192–1205.

Collin, R.W., Nikopoulos, K., Dona, M., Gilissen, C., Hoischen, A., Boonstra, F.N., Poulter, J.A., Kondo, H., Berger, W., Toomes, C., et al. (2013). ZNF408 is mutated in familial exudative vitreoretinopathy and is crucial for the development of zebrafish retinal vasculature. Proc. Natl. Acad. Sci. USA *110*, 9856–9861.

Funayama, N., Fagotto, F., McCrea, P., and Gumbiner, B.M. (1995). Embryonic axis induction by the armadillo repeat domain of beta-catenin: evidence for intracellular signaling. J. Cell Biol. *128*, 959–968.

Gal, M., Levanon, E.Y., Hujeirat, Y., Khayat, M., Pe'er, J., and Shalev, S. (2014). Novel mutation in TSPAN12 leads to autosomal recessive inheritance of congenital vitreoretinal disease with intra-familial phenotypic variability. Am. J. Med. Genet. A. *164A*, 2996–3002.

Gilmour, D.F. (2015). Familial exudative vitreoretinopathy and related retinopathies. Eye (Lond.) *29*, 1–14.

Janda, C.Y., Waghray, D., Levin, A.M., Thomas, C., and Garcia, K.C. (2012). Structural basis of Wnt recognition by Frizzled. Science *337*, 59–64.

Junge, H.J., Yang, S., Burton, J.B., Paes, K., Shu, X., French, D.M., Costa, M., Rice, D.S., and Ye, W. (2009). TSPAN12 regulates retinal vascular development by promoting Norrin- but not Wnt-induced FZD4/beta-catenin signaling. Cell *139*, 299–311.

Kashani, A.H., Brown, K.T., Chang, E., Drenser, K.A., Capone, A., and Trese, M.T. (2014a). Diversity of retinal vascular anomalies in patients with familial exudative vitreoretinopathy. Ophthalmology *121*, 2220–2227.

Kashani, A.H., Learned, D., Nudleman, E., Drenser, K.A., Capone, A., and Trese, M.T. (2014b). High prevalence of peripheral retinal vascular anomalies in family members of patients with familial exudative vitreoretinopathy. Ophthalmology *121*, 262–268.

Kaykas, A., Yang-Snyder, J., Héroux, M., Shah, K.V., Bouvier, M., and Moon, R.T. (2004). Mutant Frizzled 4 associated with vitreoretinopathy traps wild-type Frizzled in the endoplasmic reticulum by oligomerization. Nat. Cell Biol. *6*, 52–58.

Kelly, G.M., Erezyilmaz, D.F., and Moon, R.T. (1995). Induction of a secondary embryonic axis in zebrafish occurs following the overexpression of beta-catenin. Mech. Dev. *53*, 261–273.

Knoblich, K., Wang, H.X., Sharma, C., Fletcher, A.L., Turley, S.J., and Hemler, M.E. (2014). Tetraspanin TSPAN12 regulates tumor growth and metastasis and inhibits β-catenin degradation. Cell. Mol. Life Sci. *71*, 1305–1314.

Kondo, H., Kusaka, S., Yoshinaga, A., Uchio, E., Tawara, A., Hayashi, K., and Tahira, T. (2011). Mutations in the TSPAN12 gene in Japanese patients with familial exudative vitreoretinopathy. Am. J. Ophthalmol. *151*, 1095–1100 e1091.

Kühl, M., and Pandur, P. (2008). Dorsal axis duplication as a functional readout for Wnt activity. Methods Mol. Biol. *469*, 467–476.

Liebner, S., Corada, M., Bangsow, T., Babbage, J., Taddei, A., Czupalla, C.J., Reis, M., Felici, A., Wolburg, H., Fruttiger, M., et al. (2008). Wnt/beta-catenin signaling controls development of the blood-brain barrier. J. Cell Biol. *183*, 409–417.

Luhmann, U.F., Lin, J., Acar, N., Lammel, S., Feil, S., Grimm, C., Seeliger, M.W., Hammes, H.P., and Berger, W. (2005). Role of the Norrie disease pseudoglioma gene in sprouting angiogenesis during development of the retinal vasculature. Invest. Ophthalmol. Vis. Sci. *46*, 3372–3382.

MacDonald, B.T., and He, X. (2012). Frizzled and LRP5/6 receptors for Wnt/β-catenin signaling. Cold Spring Harb. Perspect. Biol. *4*, a007880.

Mao, J., Wang, J., Liu, B., Pan, W., Farr, G.H., 3rd, Flynn, C., Yuan, H., Takada, S., Kimelman, D., Li, L., and Wu, D. (2001). Low-density lipoprotein receptor-related protein-5 binds to Axin and regulates the canonical Wnt signaling pathway. Mol. Cell *7*, 801–809.

Milhem, R.M., Ben-Salem, S., Al-Gazali, L., and Ali, B.R. (2014). Identification of the cellular mechanisms that modulate trafficking of frizzled family receptor 4 (FZD4) missense mutants associated with familial exudative vitreoretinopathy. Invest. Ophthalmol. Vis. Sci. *55*, 3423–3431.

Nikopoulos, K., Gilissen, C., Hoischen, A., van Nouhuys, C.E., Boonstra, F.N., Blokland, E.A., Arts, P., Wieskamp, N., Strom, T.M., Ayuso, C., et al. (2010a). Next-generation sequencing of a 40 Mb linkage interval reveals TSPAN12 mutations in patients with familial exudative vitreoretinopathy. Am. J. Hum. Genet. *86*, 240–247.

Nikopoulos, K., Venselaar, H., Collin, R.W., Riveiro-Alvarez, R., Boonstra, F.N., Hooymans, J.M., Mukhopadhyay, A., Shears, D., van Bers, M., de Wijs, I.J., et al. (2010b). Overview of the mutation spectrum in familial exudative vitreoretinopathy and Norrie disease with identification of 21 novel variants in FZD4, LRP5, and NDP. Hum. Mutat. *31*, 656–666.

Ohlmann, A., and Tamm, E.R. (2012). Norrin: molecular and functional properties of an angiogenic and neuroprotective growth factor. Prog. Retin. Eye Res. *31*, 243–257.

Otomo, R., Otsubo, C., Matsushima-Hibiya, Y., Miyazaki, M., Tashiro, F., Ichikawa, H., Kohno, T., Ochiya, T., Yokota, J., Nakagama, H., et al. (2014). TSPAN12 is a critical factor for cancer-fibroblast cell contact-mediated cancer invasion. Proc. Natl. Acad. Sci. USA *111*, 18691–18696.

Posokhova, E., Shukla, A., Seaman, S., Volate, S., Hilton, M.B., Wu, B., Morris, H., Swing, D.A., Zhou, M., Zudaire, E., et al. (2015). GPR124 functions as a WNT7-specific coactivator of canonical β-catenin signaling. Cell Rep. *10*, 123–130.

Poulter, J.A., Ali, M., Gilmour, D.F., Rice, A., Kondo, H., Hayashi, K., Mackey, D.A., Kearns, L.S., Ruddle, J.B., Craig, J.E., et al. (2010). Mutations in TSPAN12 cause autosomal-dominant familial exudative vitreoretinopathy. Am. J. Hum. Genet. *86*, 248–253.

Poulter, J.A., Davidson, A.E., Ali, M., Gilmour, D.F., Parry, D.A., Mintz-Hittner, H.A., Carr, I.M., Bottomley, H.M., Long, V.W., Downey, L.M., et al. (2012). Recessive mutations in TSPAN12 cause retinal dysplasia and severe familial exudative vitreoretinopathy (FEVR). Invest. Ophthalmol. Vis. Sci. *53*, 2873–2879.

Qin, M., Kondo, H., Tahira, T., and Hayashi, K. (2008). Moderate reduction of Norrin signaling activity associated with the causative missense mutations identified in patients with familial exudative vitreoretinopathy. Hum. Genet. *122*, 615–623.

Savarese, M., Spinelli, E., Gandolfo, F., Lemma, V., Di Fruscio, G., Padoan, R., Morescalchi, F., D'Agostino, M., Savoldi, G., Semeraro, F., et al. (2014). Familial exudative vitreoretinopathy caused by a homozygous mutation in TSPAN12 in a cystic fibrosis infant. Ophthalmic Genet. *35*, 184–186.

Schulte, G. (2015). Frizzleds and WNT/β-catenin signaling–The black box of ligand-receptor selectivity, complex stoichiometry and activation kinetics. Eur. J. Pharmacol. *763* (*Pt B*), 191–195.

Shen, G., Ke, J., Wang, Z., Cheng, Z., Gu, X., Wei, Y., Melcher, K., Xu, H.E., and Xu, W. (2015). Structural basis of the Norrin-Frizzled 4 interaction. Cell Res. *25*, 1078–1081.

Smallwood, P.M., Williams, J., Xu, Q., Leahy, D.J., and Nathans, J. (2007). Mutational analysis of Norrin-Frizzled4 recognition. J. Biol. Chem. *282*, 4057–4068.

Stenman, J.M., Rajagopal, J., Carroll, T.J., Ishibashi, M., McMahon, J., and McMahon, A.P. (2008). Canonical Wnt signaling regulates organ-specific assembly and differentiation of CNS vasculature. Science *322*, 1247–1250.

Thiede-Stan, N.K., Tews, B., Albrecht, D., Ristic, Z., Ewers, H., and Schwab, M.E. (2015). Tetraspanin-3 is an organizer of the multi-subunit Nogo-A signaling complex. J. Cell Sci. *128*, 3583–3596.

Ulrich, F., Carretero-Ortega, J., Menéndez, J., Narvaez, C., Sun, B., Lancaster, E., Pershad, V., Trzaska, S., Véliz, E., Kamei, M., et al. (2016). Reck enables cerebrovascular development by promoting canonical Wnt signaling. Development *143*, 147–159.

van Amerongen, R., and Nusse, R. (2009). Towards an integrated view of Wnt signaling in development. Development *136*, 3205–3214.

Vanhollebeke, B., Stone, O.A., Bostaille, N., Cho, C., Zhou, Y., Maquet, E., Gauquier, A., Cabochette, P., Fukuhara, S., Mochizuki, N., et al. (2015). Tip cell-specific requirement for an atypical Gpr124- and Reck-dependent Wnt/β-catenin pathway during brain angiogenesis. eLife *4*, e06489.

Veeman, M.T., Slusarski, D.C., Kaykas, A., Louie, S.H., and Moon, R.T. (2003). Zebrafish prickle, a modulator of noncanonical Wnt/Fz signaling, regulates gastrulation movements. Curr. Biol. *13*, 680–685.

Wang, Y., Huso, D., Cahill, H., Ryugo, D., and Nathans, J. (2001). Progressive cerebellar, auditory, and esophageal dysfunction caused by targeted disruption of the frizzled-4 gene. J. Neurosci. *21*, 4761–4771.

Wang, Y., Rattner, A., Zhou, Y., Williams, J., Smallwood, P.M., and Nathans, J. (2012). Norrin/Frizzled4 signaling in retinal vascular development and blood brain barrier plasticity. Cell *151*, 1332–1344.

Xia, C.H., Liu, H., Cheung, D., Wang, M., Cheng, C., Du, X., Chang, B., Beutler, B., and Gong, X. (2008). A model for familial exudative vitreoretinopathy caused by LPR5 mutations. Hum. Mol. Genet. *17*, 1605–1612.

Xu, Q., Wang, Y., Dabdoub, A., Smallwood, P.M., Williams, J., Woods, C., Kelley, M.W., Jiang, L., Tasman, W., Zhang, K., and Nathans, J. (2004). Vascular development in the retina and inner ear: control by Norrin and Frizzled-4, a high-affinity ligand-receptor pair. Cell *116*, 883–895.

Yang, H., Xiao, X., Li, S., Mai, G., and Zhang, Q. (2011). Novel TSPAN12 mutations in patients with familial exudative vitreoretinopathy and their associated phenotypes. Mol. Vis. *17*, 1128–1135.

Ye, X., Wang, Y., Cahill, H., Yu, M., Badea, T.C., Smallwood, P.M., Peachey, N.S., and Nathans, J. (2009). Norrin, frizzled-4, and Lrp5 signaling in endothelial cells controls a genetic program for retinal vascularization. Cell *139*, 285–298.

Zhou, Y., and Nathans, J. (2014). Gpr124 controls CNS angiogenesis and blood-brain barrier integrity by promoting ligand-specific canonical wnt signaling. Dev. Cell *31*, 248–256.

Zhou, Y., Wang, Y., Tischfield, M., Williams, J., Smallwood, P.M., Rattner, A., Taketo, M.M., and Nathans, J. (2014). Canonical WNT signaling components in vascular development and barrier formation. J. Clin. Invest. *124*, 3825–3846.